

UNIVERSITY OF PARDUBICE
FACULTY OF CHEMICAL TECHNOLOGY
Department of Inorganic Technology

Petr Klein

**NMR Spectroscopy of Cations in Extra-framework Sites
in Zeolites**

Theses of the Doctoral Dissertation

Pardubice 2018

Study program: **Chemistry and Chemical Technology**
Study field: **Inorganic Technology**

Author: **Ing. Petr Klein**
Supervisor: **Mgr. Jiří Dědeček, CSc., DSc.**
Year of the defence: 2018

References

KLEIN, Petr. *NMR Spectroscopy of Cations in Extra-framework Sites in Zeolites*. Pardubice, 2018. 109 pages. Dissertation thesis (PhD.). University of Pardubice, Faculty of Chemical Technology, Department of Inorganic Technology. Supervisor Mgr. Jiří Dědeček, CSc., DSc.

Abstract

This thesis deals with the application of advanced methods of solid-state nuclear magnetic resonance (NMR) spectroscopy to determine the extra-framework positions of selected alkali metal cations in zeolites.

One objective was to develop a procedure allowing to distinguish crystallographic positions of Li^+ and Na^+ cations in silicon-rich zeolites and to verify applicability of quantum chemical calculations for interpretation of NMR spectra. The zeolite of FER structure type was chosen as a model system. Based on the complex analysis of the set of synthetic FER zeolites using ^{27}Al NMR, ^{29}Si NMR and UV-Vis spectroscopy, three samples with different distribution of Al in the framework were selected. Their dehydrated lithium- and sodium- exchanged forms were subsequently investigated by solid-state NMR techniques under magic angle spinning (MAS).

A two-dimensional ^7Li - ^7Li exchange correlation spectroscopy (EXSY) NMR experiment was used for the first time to distinguish non-equivalent Li^+ crystallographic positions in a narrow range of chemical shifts. The relative concentration of Li^+ at the individual positions was subsequently determined by the deconvolution of the one-dimensional ^7Li MAS NMR spectra. To distinguish broad quadrupolar resonances of different Na^+ sites and to obtain their NMR parameters, it was necessary to simultaneously analyze one-dimensional ^{23}Na MAS NMR and two-dimensional multi-quantum (MQ) MAS NMR spectra measured on two different magnetic fields (high and ultra-high field). Quantum-chemical calculations were employed to interpret NMR spectra. The calculated NMR parameters were in good agreement with the experimental values and allowed interpretation of NMR spectra. However, little to no difference between the calculated parameters of several sites does not allow unambiguous assignment of all resonances to particular extra-framework site. Therefore, knowledge of Al distribution in the framework is of high interest.

Another objective was to verify the possibility of analyzing the structure of the cationic position indirectly by ^{27}Al MAS NMR using the influence of the cation on the coordination of Al in the dehydrated zeolite. For this purpose a zeolite of CHA structure type, which contains only one type of framework Al site was chosen. Both hydrated and dehydrated lithium-, sodium-, and potassium- exchanged forms of zeolite CHA were investigated using ^{27}Al MAS and MQMAS NMR. Significant broadening of ^{27}Al NMR spectra of dehydrated samples was observed, depending on the ionic radius of the extra-framework cation. The analysis of this broadening provides additional structural information on the extra-framework positions of cations in zeolites, including K^+ , which is difficult to measure. Theoretical calculations have shown that enlargement is primarily caused by deformation of AlO_4^- , due to cation binding.

Abstrakt

Tato práce se zabývá aplikací pokročilých metod spektroskopie nukleární magnetické rezonance (NMR) pevné fáze pro určení mimo-mřížkových poloh vybraných jednomocných kationtů alkalických kovů v zeolitech.

Jedním z cílů bylo vytvoření postupu pro rozlišení jednotlivých krystalografických poloh kationtů Li^+ a Na^+ v zeolitech s vysokým obsahem křemíku, včetně ověření možnosti interpretace NMR spekter pomocí kvantově chemických výpočtů. Jako modelový systém byl zvolen zeolit strukturního typu FER. Na základě komplexní analýzy sady syntetických FER zeolitů pomocí ^{27}Al NMR, ^{29}Si NMR a UV-Vis spektroskopie byly vybrány tři vzorky s rozdílnou distribucí Al ve skeletu. Jejich dehydratované lithné a sodné formy byly následně zkoumány pomocí NMR technik pevné fáze za rotace vzorku pod magickým úhlem (MAS).

Pro rozlišení neekvivalentních krystalografických poloh Li^+ v úzkém rozsahu chemických posunů byl poprvé použit dvourozměrný ^7Li - ^7Li výměnný korelační (EXSY) NMR experiment. Relativní zastoupení Li^+ v jednotlivých polohách bylo následně určeno pomocí dekonvoluce jednorozměrného ^7Li MAS NMR spektra. Pro rozlišení kvadrupolárně rozšířených signálů jednotlivých poloh Na^+ bylo nutné souběžně analyzovat jednorozměrná ^{23}Na MAS NMR a dvourozměrná vícekvantová (MQ) MAS NMR spektra změřená na dvou různých magnetických polích (vysokém a ultra-vysokém). Pro interpretaci NMR spekter byly použity kvantově-chemické výpočty. Vypočtené NMR parametry byly v dobrém souladu s experimentálními hodnotami, avšak podobnost vypočtených parametrů některých kationtových poloh neumožnila jejich dostatečné rozlišení bez znalosti distribuce Al ve skeletu.

Dalším z cílů bylo ověření možnosti analýzy struktury kationtové polohy nepřímo pomocí ^{27}Al MAS NMR s využitím vlivu kationtu na koordinaci Al v dehydratovaném zeolitu. K tomu byl vybrán zeolit strukturního typu CHA, který obsahuje pouze jednu mřížkovou polohu Al. Jeho lithná, sodná a draselná forma byla zkoumána v hydratovaném i dehydratovaném stavu pomocí ^{27}Al MAS a MQMAS NMR experimentů. Bylo zjištěno znatelné rozšíření Al spekter dehydratovaných vzorků v závislosti na iontovém poloměru mimomřížkového kationtu. Analýza tohoto rozšíření přináší další strukturní informace o mimo-mřížkových polohách kationtů v zeolitech, a to včetně K^+ , které je obtížně měřitelné. Teoretické výpočty prokázaly, že příčinou rozšíření je především deformace AlO_4^- , která je způsobena navázáním kationtu.

Keywords

zeolite, solid-state NMR spectroscopy, framework Al site, extra-framework cations, ferrierite, chabazite, heterogeneous catalysis

Klíčová slova

zeolit, NMR spektroskopie pevné fáze, mřížková poloha Al, mimomřížkové kationty, ferrierit, chabazit, heterogenní katalýza

Table of Contents

INTRODUCTION	6
1 ZEOLITES IN HETEROGENEOUS CATALYSIS	6
1.1 Analysis of Extra-framework Cations in Zeolites	7
2 SOLID-STATE NMR SPECTROSCOPY	8
2.1 Application of ssNMR for Investigation of Extra-Framework Cations in Zeolites	8
2.1.1 Lithium ssNMR	8
2.1.2 Sodium ssNMR	9
2.1.3 Aluminium ssNMR	9
2.2 Interpretation of ssNMR Spectra	9
3 AIM OF STUDY	10
4 MATERIALS AND METHODS	10
4.1 Samples Preparation	10
4.2 Solid-State NMR experiments	11
5 RESULTS AND DISCUSSION	12
5.1 Lithium ssNMR of Li-FER samples	12
5.2 Sodium ssNMR of Na-FER samples	17
5.3 Structure of cationic sites in dehydrated CHA as seen by ²⁷ Al ssNMR	19
CONCLUSIONS	22
LIST OF REFERENCES	23
LIST OF STUDENTS' PUBLISHED WORKS	27

Introduction

Zeolites are microporous crystalline aluminosilicates, which represent an important group of inorganic materials in modern chemistry. Zeolite structure is formed by SiO_4 and AlO_4^- (generally TO_4) tetrahedra sharing oxygens in their corners. The three-dimensional framework of linked tetrahedra forms well-organized microporous system of channels and interconnected cavities with thousands of possible arrangements. Up to date, 239 framework type codes have been assigned.¹ Zeolites occur as natural minerals, but are also synthesized and produced industrially. Because of the unique combination of the properties, such as large surface area, well organized micropore channel system, presence of exchangeable cationic species, high chemical and thermal stability, zeolites are used in a variety of applications with a global market of several million tones per year.² There are three main commercial applications of zeolites: in detergents, in separation and absorption, and in catalysis. The largest application in volume is in detergents, but with respect to the financial market and industrial impact, catalysis is the largest application of zeolites.² In the case of catalysis mostly the synthetic zeolites are used, since their properties for the specific reactions and processes can be controlled by tuning synthesis parameters.

The knowledge of the relationship between chemical composition, structural parameters, and chemical and physical properties of the material in a particular process is essential. Solid-state nuclear magnetic resonance (ssNMR) spectroscopy represents one of the most powerful analytical methods for determining the structural properties at the atomic level. This method allows a unique view of coordinating state and chemical environment of individual atoms. This work deals with the applications of ssNMR supported by quantum chemical calculations for the analysis of crystallographic positions of monovalent extra-framework cations in zeolite with low relative concentration of aluminium in the framework.

1 Zeolites in Heterogeneous Catalysis

Zeolites have the ability to act as catalysts for chemical reactions taking place within the internal channels and cavities. The isomorphous substitution of Si^{IV} atoms by the Al^{III} ones introduces negative charge into the silicate framework and has to be compensated by positively charged ions or protons. These cationic species occupy extra-framework positions in the zeolite channels and can play a role of reaction/sorption centers (active sites) accessible for various molecules.

Due to flexible chemical composition is possible to control the type, number and strength of active sites as well as the adsorption properties. Silicon-rich zeolites have outstanding thermal and hydrothermal stability making their regeneration easy and repeatable. Zeolites are frequently referred as “green catalysts”.³

Aluminum-rich zeolites (Si/Al 1 - 4) with faujasite (FAU) structure are the most common zeolites used in heterogeneous catalysis. Nevertheless, in recent thirty years, the application of silicon-rich zeolites ($\text{Si}/\text{Al} > 8$) arises. ZSM-5, beta zeolite, MCM-22, mordenite and ferrierite are the silicon-rich zeolites with the highest industrial impact.^{4,5} An important class of reactions is catalyzed by protonic form of zeolites, whose framework-bound protons give rise to very high acidity. This is utilized in many industrial application in oil refining and petrochemistry, including

crude oil cracking (fluid catalytic cracking - FCC, hydrocracking), isomerization and alkylation of paraffins/olefins, conversion of methanol to hydrocarbons (methanol to gasoline - MTG, methanol to light olefins – MTO).^{4, 6-9}

Zeolites containing transition metal ions in extra-framework positions represent group of redox catalysts. They found applications in the abatement of NO_x from diesel engine exhaust gases and in nitric acid plants.¹⁰⁻¹²

There are also many promising application in hydrocarbon syntheses, synthesis of fine chemicals,^{3, 13} biomass conversion,¹⁴ the conversion of methane to form more valuable products (such as methanol and benzene)¹⁵ and carbon dioxide utilization and abatement.¹⁶

Zeolitic materials where Al is replaced by other isomorphously substituted metal exhibit unique properties as demonstrated in the use of titanium silicate TS-1 in the production of caprolactam and in the oxidation of benzene to phenol by nitrous oxide (BTOP reaction).¹⁷⁻¹⁹

These developments and related successes have only been possible by increased knowledge and related technological advances in the tailoring of zeolite-based catalysts. In the last decades we have seen an expanding scientific base, often obtained by a synergistic approach between experiment and theory, for the advanced synthesis and use of zeolites. The design of advanced catalytic systems exhibiting high activity and selectivity and meeting requirements on industrial applications represents a complex process which can hardly be finalized without the detailed knowledge of the structure of the active sites and their distribution in the molecular sieve.

1.1 Analysis of Extra-framework Cations in Zeolites

The physico-chemical properties of zeolites are strongly related to the crystal structure. The key information is not only in the structure type, but also in the distribution of the aluminium and derived distribution of the cations in extra-framework positions in the zeolite cavities and channels. Since the distribution of the cations controls the electric fields, the characterization of the cation sites is a prerequisite for understanding of the physical properties of zeolites.²⁰ Basic spectroscopic method for analysis of structure parameters and cation siting is X-ray diffraction (XRD). In aluminium-rich zeolites extra-framework sites of different cations (except lithium) are very well described by XRD in the number of publications and are compiled by Mortier²¹ for the most common structure types.

Contrary to Al-rich zeolites, publications on cation siting in Si-rich zeolites are less numerous. Diffraction studies of cations in extra-framework positions in silicon-rich zeolites meet extreme difficulties due to the low concentration of active sites, large unit cells with a low symmetry, and a high number of different local structures accommodating cationic sites and often having several close structures. In pioneer work by Olson et al.²², synchrotron diffraction was used to characterize Cs⁺ in ZSM-5. Mentzen²³ analyzed H-, Li-, Na-, K-, Rb-, and Tl-ZSM-5 using synchrotron a neutron diffraction. Dalconi and co-workers identified only 3 different cobalt sites in dehydrated ferrierite (Co-FER with Si/Al 8,5) by XRD and EXAFS²⁴ and 4 cationic sites in dehydrated zeolite Ni-FER with the Si/Al 8,5 by powder XRD.²⁵ Seff²⁶ characterized Cs⁺ sites in single crystal of ZSM-5 using synchrotron diffraction. Dědeček et al.^{27, 28} analyzed Co²⁺ siting in hydrated and dehydrated Si-rich zeolites by

a UV-Vis diffuse reflectance spectroscopy. Analysis of accessibility and nature of active sites by adsorption of probe molecules and monitored using combination of FTIR and DFT calculations was reviewed by Nachtigall.²⁹ Important method for characterization of cations and adsorbed molecules in zeolites reveals solid-state NMR spectroscopy.

2 Solid-state NMR Spectroscopy

Solid-state NMR spectroscopy is a powerful tool for a structural characterization which is not affected by the issues causing difficulties in diffraction studies as discussed above. A high sensitivity of ssNMR techniques for chemical bonds in the local structure of the resonating nuclei is utilized for characterization of framework atoms, extra-framework species, surface sites, and adsorbate complexes in zeolites with great success. Many atoms occurring in zeolites possess isotopes with a nuclear spin, which makes these isotopes NMR-active. ¹¹B, ¹⁷O, ²⁷Al, ²⁹Si, ³¹P, ⁵¹V, ⁶⁷Zn, and ⁷¹Ga isotopes are accessible for NMR spectroscopy and contribute to the framework of zeolites in a broad manner. ¹H, ⁷Li, ²³Na, and ¹³³Cs isotopes are interesting for the characterization of surface OH groups and extra-framework species, such as extra-framework cations.³⁰

2.1 Application of ssNMR for Investigation of Extra-Framework Cations in Zeolites

Lithium and sodium are important extra-framework species in zeolites. Solid-state NMR spectroscopy is the suitable method for investigating the distribution and coordination of lithium and sodium cations in zeolites. Although these nuclei have a spin $I > 1/2$ (⁶Li: spin $I = 1$; ⁷Li: spin $I = 3/2$; ²³Na: spin $I = 3/2$), only the quadrupolar interaction of ²³Na nuclei causes a dominating line broadening effect.³⁰

2.1.1 Lithium ssNMR

Lithium exchanged zeolites represent promising material for CO₂ capture. Thanks to its small diameter it is promising probe for Al siting in zeolites.

Both the lithium nuclides ⁶Li and ⁷Li are useable for NMR spectroscopy. In the most cases of the investigation of lithium-exchanged zeolites by solid-state NMR spectroscopy, the spin $I = 3/2$ ⁷Li nucleus is studied, since it has a significantly higher natural abundance in comparison with the spin $I = 3/2$ ⁶Li nucleus (⁶Li: 7.42%, ⁷Li: 92.58%) and favorable receptivity. In some cases ⁶Li spectra can be useful. Because of the weak quadrupole moment of ⁷Li nuclei ($Q = -4.01 \times 10^{-30} \text{ m}^2$), the ⁷Li MAS NMR spectra of lithium cations in hydrated as well as dehydrated zeolites consist of narrow isotropic lines.³⁰

However, individual resonances of lithium are in the small range of chemical shift, making analysis of Li⁺ siting in Si-rich zeolites with number of distinguishable T-atoms complicated. Thus, it is necessary to setup experiments for maximal possible resolution.

2.1.2 Sodium ssNMR

Due to the large quadrupole moment of ^{23}Na nuclei ($Q = 10.4 \times 10^{-30} \text{m}^2$)³¹, the MAS NMR spectra of sodium cations in dehydrated zeolites are dominated by broad quadrupolar patterns. The overlap of the ^{23}Na MAS NMR signals of sodium cations located on crystallographically non-equivalent extra-framework positions makes the separation and assignment of the corresponding signals difficult and requires field-dependent experiments^{32, 33} or application of MQMAS techniques^{20, 34-36}. Utilizing the above-mentioned experimental techniques, the quadrupole coupling constant C_Q , the asymmetry parameter η_Q , and the isotropic chemical shift δ can be obtained.³⁰

2.1.3 Aluminium ssNMR

The ^{27}Al MAS NMR experiments on hydrated zeolites allowed a determination of the siting of Al atoms in the T sites³⁷ but the local arrangement of the whole cationic site (i.e., the extra-framework cation and the framework atoms forming the structure of the cationic site including the balanced framework Al atoms) could not have been analyzed. Only a few studies investigated dehydrated zeolites by ^{27}Al MAS NMR spectroscopy and therefore our knowledge in this area is significantly limited.^{38, 39} Freude et al. demonstrated that it was possible to monitor Al atoms in dehydrated zeolites by ^{27}Al MAS NMR spectroscopy and his results showed a variability of the ^{27}Al MAS NMR spectra and line widths for faujasite and ZSM-5 structures exchanged with Na and H cations.³⁸⁻⁴¹ Thus, the ^{27}Al NMR spectra of dehydrated zeolites have to contain complex and detailed information regarding the Al siting in the framework and concerning the local structure of the site accommodating the extra-framework cation in a dehydrated zeolite. However, this information has not been utilized yet. This is caused by the absence of understanding the mechanism of the broadening of the spectra and of the parameters controlling its width and shape.

2.2 Interpretation of ssNMR Spectra

Simulations of site arrangements using *ab-initio* quantum chemistry methods followed by predictions of NMR parameters of the involved atoms represent an essential part of the interpretation of ssNMR spectra as there is not an empirical method of the interpretation of the NMR results at an atomic level. A variety of methods, such as Hartree-Fock (HF), density functional theory (DFT) and the gauge-including projector augmented-wave (GIPAW) have been used to predict the NMR tensor parameters.^{42, 43} Generally, at first the probable position of given species have to be find (or defined). In the case of Al, the position in given T site is known from XRD measurements. For cations, extra-framework position has to be calculated by molecular dynamics using density function theory (DFT). Subsequently, the local structure of the given species has to be optimized by periodic DFT or in some cases by quantum mechanics/molecular mechanics approach (QM/MM). Afterwards NMR parameters for optimized structure are calculated and therefore individual resonances in the NMR spectrum can be assigned to given species.

3 Aim of Study

The aim of this study is to employ techniques of solid-state NMR spectroscopy for analysis of crystallographic positions of monovalent cations in zeolites with focus on following objectives:

- Development of methods and methodology to increase the resolution of NMR experiments necessary for the analysis of cation siting in silicon-rich zeolites.
- Verification of reliability of quantum chemical calculation of NMR parameters of non-relativistic nuclei of monovalent cations in cationic sites in zeolites.
- Analysis of siting and coordination of Li^+ and Na^+ ions in zeolite of selected structure.
- Application of monovalent cations monitored by NMR as supplementary method for the analysis of Al siting in silicon-rich zeolites.
- To test possibility and develop methods and methodology for indirect characterization of siting of monovalent cations including “NMR invisible” in zeolites via analysis of local arrangement of framework Al atoms in dehydrated zeolites.

4 Materials and Methods

As a model material for testing and verification of methods and procedures suitable for analysis of extra-framework sites in silicon-rich zeolites, FER framework type was chosen. One of the reasons is presence of four framework T sites, which one of the lowest number among silicon-rich structures. Moreover, it is available in a range of Si/Al ratios and it can be synthesized by different routes.

In a preliminary study, 5 different zeolites of FER structure were analyzed. Complex multi-spectroscopic approach using ^{29}Si NMR and UV-Vis spectroscopy and ^{27}Al MQMAS NMR interpreted by periodic DFT allowed determination of aluminium siting in the FER framework.³⁷ Three of them containing mostly isolated Al atom were used for further analysis of extra-framework sites.

To elucidate an effect of cation on ^{27}Al NMR spectra of zeolites, zeolite of CHA framework were investigated, as it contains only one framework T site and low Si/Al ratio allow acquisition of Al NMR spectra on reasonable timescale.

4.1 Samples Preparation

The parent FER/20 (FER/A in Ref.³⁷) sample with Si/Al of 20 was purchased from Unipetrol, a.s., Czech Republic. The parent FER/27 sample (Si/Al 30, FER/B in Ref.³⁷) was synthesized using pure silica (Cab-O-Sil M5), sodium and aluminum

sulfate and NaOH. Pyridine served as the structure directing agent. The parent FER/30 sample (Si/Al 30, FER/C in Ref.³⁷) was purchased from Zeolyst International, Inc. The parent CHA sample with Si/Al of 2.4 was prepared according to the procedure described in Ref.⁴⁴

The parent samples were ion-exchanged with 0.5 M NH_4NO_3 twice for 24 hours to obtain the NH_4 -forms. Then the NH_4 -forms of parent zeolites were ion-exchanged into the M-FER (M = Li, Na) and M-CHA (M = Li, Na, and K) forms by repeated (3×24 hours) M^+ ion-exchange using 0.5 M MNO_3 (50 ml per 1 g of a zeolite) at 70°C for Li^+ and at room temperature for Na^+ and K^+ . Subsequently, samples were filtered, thoroughly washed with distilled water and then equilibrated on air at room temperature to guarantee their full hydration.

For analysis of cations in extra-frameworks positions, cationic forms of zeolites were dehydrated to enable coordination of cations to the zeolite framework. Prior to the dehydration, hydrated samples were packed into the ZrO_2 MAS NMR rotors and dried overnight in the oven at 100°C to remove excess water. The dehydrated samples for the NMR experiments were prepared “*in situ*” using instrumental setup developed in this work to allow dehydration and subsequent sealing of the cooled samples in NMR rotors under vacuum. Samples were dehydrated at 450°C under dynamic vacuum of $p = 1.10^{-1}$ Pa for 3 hours with a heating ramp of 3°C min^{-1} . Subsequently to the dehydration, the samples were cooled down at room temperature and airtight-sealed with Kel-F cups. Sealed rotors were immediately transferred into the glass tubes, which were evacuated and heat-sealed to prevent rehydration of the samples before NMR measurements.

4.2 Solid-State NMR experiments

Solid-state NMR experiments were carried out in the Joint Laboratory of Solid-State NMR, Institute of Macromolecular Chemistry, AS CR and Jaroslav Heyrovský Institute of Physical Chemistry, AS CR on a Bruker Avance III HD 500 WB/US three-channel NMR spectrometer equipped with a wide bore ultra-stabilized magnet charged to $B_0 = 11.7$ T ($\nu_0(^1\text{H}) = 500$ MHz) adapted for measuring of high resolution NMR spectra of solid samples. An external cooling unit and set of NMR probe heads allow performing NMR experiments under wide range of experimental conditions. In this work, solid state NMR spectra were measured using either 4 mm or 3.2 double resonance probe heads. Samples packed in the ZrO_2 rotors with outer diameter of either 4 mm or 3.2 mm and sealed with Kel-F caps were spun under magic angle at spinning frequencies of 7-22 kHz.

A set of dehydrated Na-FER samples were measured on a Bruker Avance II 4-channel NMR spectrometer equipped with a narrow bore ultra-stabilized 21.1 T ($\nu_0(^1\text{H}) = 900.08$ MHz) magnet using a 4 mm double-resonance MAS probe-head (Bruker, 4 mm, 18 kHz MAS, $1\text{H}/^{13}\text{C}/^{15}\text{N}$, CP/MAS, VT) at the National Ultrahigh-Field NMR Facility for Solids in Ottawa, Canada.

^7Li ssNMR spectra were acquired at Larmor frequency $\nu_0(^7\text{Li}) = 194.37$ MHz using either a 4 mm or a 3.2 mm double-resonance MAS probe-heads at spinning frequencies of $\nu_{\text{rot}} = 12$ kHz and $\nu_{\text{rot}} = 20$ kHz, respectively. The two-dimensional single quantum ^7Li - ^7Li exchange correlation (EXSY) NMR spectra were recorded using the optimized NOESY-type three-pulse sequence. The quantitative

one-dimensional ^7Li MAS NMR spectra were acquired using the optimized single pulse excitation with an optional proton decoupling. The ^7Li chemical shift was referenced externally to 1M solution of LiCl by the signal of solid LiCl at $\delta_{\text{iso}} = -1.04$ ppm.

^{23}Na ssNMR experiments were carried out at two different external magnetic fields at Larmor frequencies $\nu_0(^{23}\text{Na}) = 132,3$ MHz and $\nu_0(^{23}\text{Na}) = 238,1$ MHz using a 3.2 mm and 4 mm double-resonance MAS probes, respectively. The quantitative one-dimensional ^{23}Na MAS NMR spectra were collected using optimized single pulse excitation with optional high-power proton decoupling. The two-dimensional ^{23}Na MQMAS NMR spectra were recorded using optimized z-filtered three-pulse sequence. The ^{23}Na chemical shifts were referenced externally to 1M solution of NaCl by using the signal of solid NaCl at 7.2 ppm.

The quantitative ^{27}Al MAS NMR spectra were recorded using optimized single pulse excitation at the rotation frequency of 12 kHz and 20 kHz for the hydrated and dehydrated samples, respectively. The two-dimensional triple-quantum ^{27}Al 3Q MAS NMR spectra of the dehydrated M-CHA samples were recorded using optimized z-filtered three-pulse sequence. The ^{27}Al chemical shifts were referenced to 1M solution of $\text{Al}(\text{NO}_3)_3$ by using signal of solid $\text{Al}(\text{NO}_3)_3$ at 0.0 ppm as an external reference.

Analytical simulations of NMR spectra were performed using dmfit⁴⁵ program. This software allows modeling of powder patterns of a broad range of NMR active nuclei in various types of experiments using a set of model functions and thus allows obtain NMR parameters of individual resonances.

5 Results and Discussion

5.1 Lithium ssNMR of Li-FER samples

To investigate lithium environment, three dehydrated Li-FER samples were studied by ^7Li MAS NMR spectroscopy. One-dimensional lineshapes (see Figure 1) contain close overlapping resonances in a narrow range of chemical shifts with negligible quadrupolar broadening. To identify individual resonances high resolution ^7Li - ^7Li homonuclear correlation MAS NMR spectroscopy was implemented. By careful analysis of cross sections of 2D correlation spectra (see Figure 2) six lithium resonances were found in Li-FER samples. These were used in models to fit ^7Li MAS NMR spectra (see Figure 1) to obtain quantitative distribution of Li^+ . The ^7Li chemical shifts of individual lithium resonances and corresponding relative concentration of Li^+ ions in crystallographically non-equivalent extra-framework positions in Li-FER samples are summarized in Table 1.

Table 1 - ^7Li chemical shift (δ) and relative intensity (I) of individual Li^+ resonances in dehydrated Li-FER samples

sample	^7Li NMR resonance											
	R1		R2		R3		R4		R5		R6	
	δ/ppm	I/%	δ/ppm	I/%	δ/ppm	I/%	δ/ppm	I/%	δ/ppm	I/%	δ/ppm	I/%
Li-FER/20			-0.23	40			-0.80	50	-1.07	10		
Li-FER/27	0.17	5	-0.20	15			-0.80	60	-1.05	20		
Li-FER/30	0.12	5			-0.55	72	-0.85	20			-1.50	3

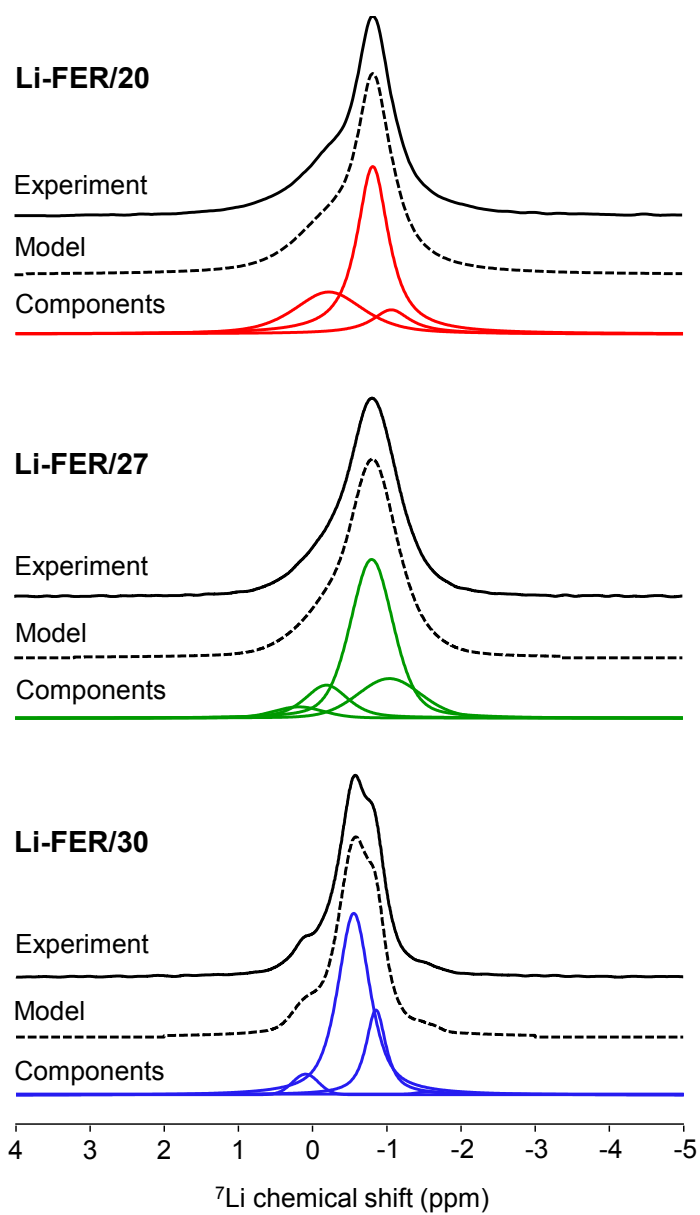


Figure 1 - Experimental and modeled ^7Li MAS NMR spectra of Li-FER samples

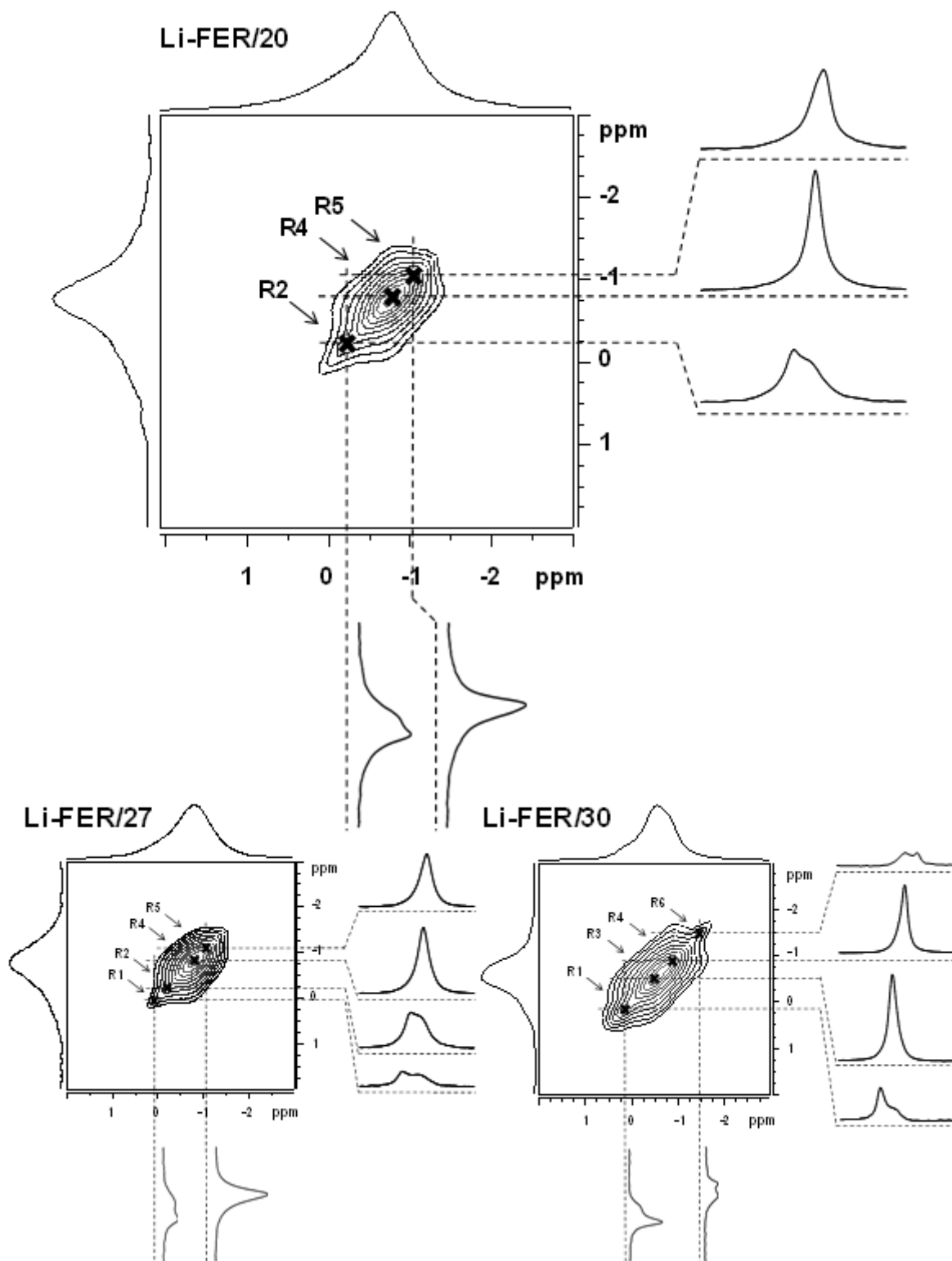


Figure 2 - ${}^7\text{Li}$ - ${}^7\text{Li}$ homonuclear correlation spectra of Li-FER samples together with skyline projections, selected cross sections, and marked positions of lithium resonances R1-R6

For interpretation of ^7Li MAS NMR spectra quantum-chemistry computations were employed. Theoretical computations were made by group of Dr. Štěpán Sklenák (see Ref.⁴⁶ for details). Six optimized structures of the low energy Li^+ sites (two sites denoted as T1A and T1B for Li^+ balancing Al in T1 site, T2A and T2B for Al(T2), T3 for Al(T3), and T4 for Al(T4)) with calculated values of lithium chemical shifts and the relative energies of are listed in Table 2.

Table 2 - Calculated ^7Li chemical shifts (δ_{calc}) and relative energies (ΔE) of six optimized low energy Li^+ sites

Li^+ site	δ_{calc} ppm	ΔE kcal/mol
T1A	0.32	0.0
T1B	-0.34	0.9
T2A	-0.86	0.0
T2B	-0.45	0.2
T3	-0.78	0.0
T4	-0.71	0.0

The experimental ^7Li chemical shifts of lithium resonances are compared with the calculated values in Figure 4. The pattern of the experimental and calculated ^7Li chemical shifts shows significant similarities, thus, we were able to assign lithium structures to individual resonances (see Figure 4). An assignment of such close resonances has to be performed very carefully but still resonances T3 and T4 cannot be distinguished. There are no experimental data based on diffraction methods regarding the siting of Li^+ in ferrierites.

However, the knowledge of the Al siting in the three ferrierite samples used in Ref.³⁷ permits a verification of the siting of Li^+ ions obtained in this study. The Al atoms occupy the T sites in the samples (for details see Figure 6 of Ref.³⁷) as follows: T2, T3, and T4 in FER/20; T1, T2, T3, and T4 in FER/27; and T1, T3, and T4 in FER/30.

Figure 4 compares the relative concentration of Al atoms (in %) corresponding to the T sites obtained from (i) the corresponding Li^+ siting analyzed using ^7Li MAS NMR and (ii) ^{27}Al MAS NMR experiments.

The agreement between the results obtained by ^7Li and ^{27}Al MAS NMR is very good and confirms the assignment of the experimental ^7Li NMR resonances to the Li^+ sites related to Al in the individual T sites. It opens possibility to use Li as an additional probe of Al siting and shows importance and usefulness of multinuclear NMR approach.

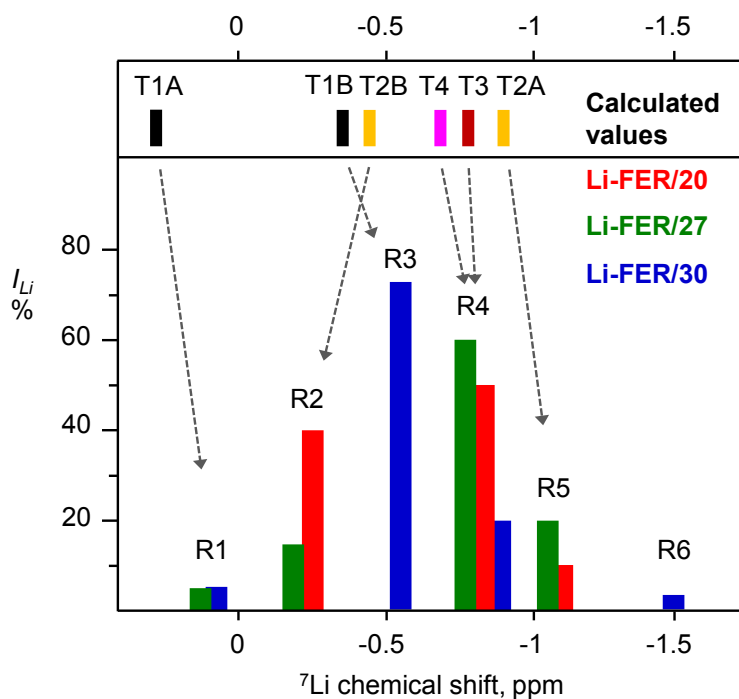


Figure 3 - Experimental ${}^7\text{Li}$ chemical shifts of Li^+ resonances and their intensities in the spectra of the dehydrated Li-FER samples, ${}^7\text{Li}$ chemical shifts calculated for Li^+ ions balancing Al atoms in the T1- T4 sites, and their assignments to the experimental data. Li-FER/20 (■), Li-FER/27 (■), and Li-FER/30 (■); Li^+ balancing Al in the T1 (■), T2 (■), T3 (■), and T4 (■) sites

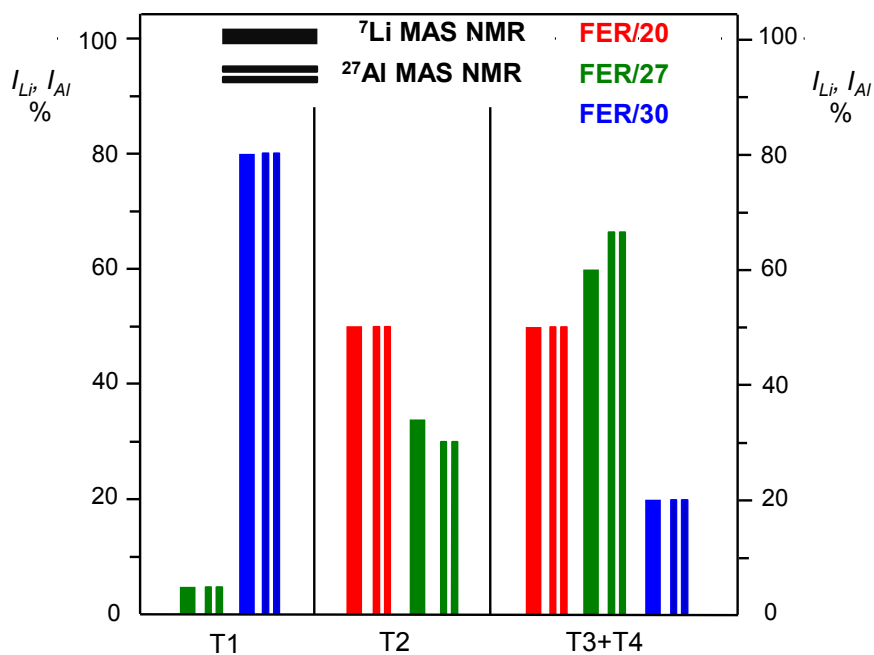


Figure 4 - Relative concentration of Al atoms (in %) corresponding to the distinguishable framework T sites obtained from (i) the corresponding Li^+ siting analyzed using ${}^7\text{Li}$ MAS NMR and (ii) ${}^{27}\text{Al}$ MAS NMR³⁷

5.2 Sodium ssNMR of Na-FER samples

^{23}Na MAS and MQMAS NMR spectra of dehydrated Na-FER samples were acquired at both high and ultra-high magnetic field strengths of 11.7 T (500 Hz) and 21.1 T (900 Hz), respectively (see spectra of Na-FER/30 in Figure 5).

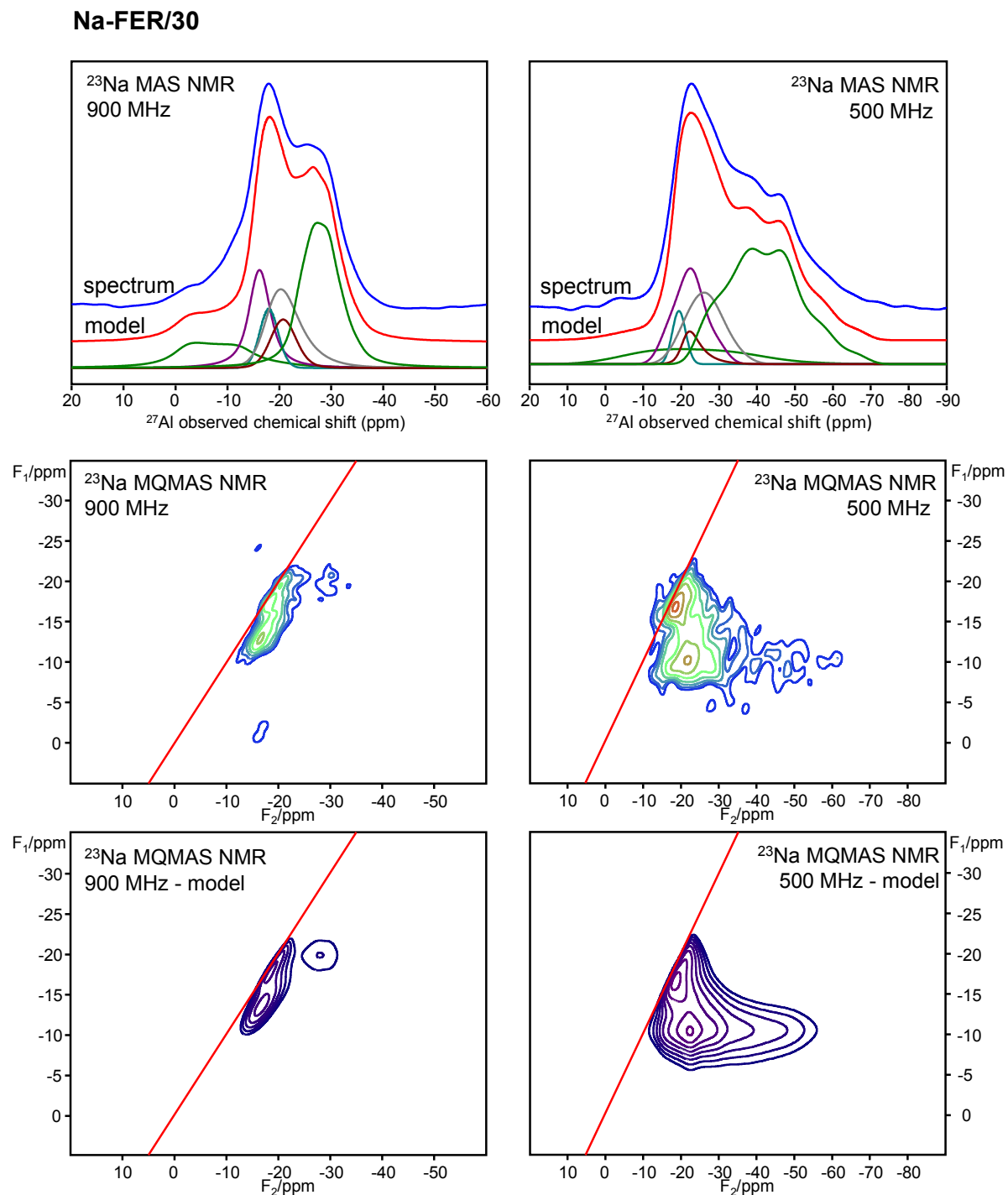


Figure 5 - Experimental and modeled ^{23}Na MAS and MQMAS NMR spectra of Na-FER/30 sample recorded at $B_0 = 11.7$ T (500 Hz) and $B_0 = 21.1$ T (900Hz)

^{23}Na NMR experiments at 11.7 T did not allow complete analysis of Na^+ environment in our samples because some resonances found in ^{23}Na MAS NMR spectra were not observed in MQMAS spectra. Moreover, experiments are very time consuming and resulting spectra are very broad due to the strong quadrupolar interaction. In contrast to ^{23}Na NMR experiments at 11.7 T, measurements performed at ultra-high magnetic field of 21.1 T provide much better results regarding spectral resolution and time consumption. Even the signal to noise ratio of MQMAS experiments at 21.1 T is similar to those at 11.7 T, spectral resolution increased due to the suppression of quadrupolar broadening. By careful simultaneous modeling of MAS and MQMAS spectra recorded at 11.7 T and 21.1 T (i.e. analysis of 4 spectra at once for each sample), 4-6 resonances were found in Na-FER samples and their NMR parameters were extracted. An example of the best fit of Na-FER/30 sample is shown in Figure 5. Experimental values of chemical shift and quadrupolar coupling constant of Na^+ resonances taken from model of ^{23}Na MAS NMR spectra recorded at 21.1 T are summarized in Table 3 and displayed graphically in Figure 6.

Table 3 - ^{23}Na chemical shift (δ_{Na}), quadrupolar constant (C_Q) and relative intensity (I) of individual Na^+ resonances of Na-FER samples

sample	res.	$\delta_{\text{Na}}/\text{ppm}$	C_Q/MHz	I/%	Na^+ site
Na-FER/20	I	0.0	4.7	15	T2-/T4-6MR
	IIa	-15.6	2.1	31	T3-8MR2
	IIb	-19.2	2.0	15	T4-8MR
	III	-22.5	3.6	39	T1-/T2-8MR1
Na-FER/27	I	-1.0	4.4	10	T2-/T4-6MR
	IIa	-15.5	2.2	53	T3-8MR2
	IIb	-19.0	2.1	11	T4-8MR
	III	-22.0	3.6	26	T1-/T2-8MR1
Na-FER/30	I	2.0	4.7	13	T2-/T4-6MR
	IIa	-14.2	2.0	16	T1-8MR2
	IIb	-17.5	1.0	7	T3-8MR
	IIc	-18.0	2.3	18	T4-8MR
	IId	-20.0	1.3	8	T1-ALPH
	III	-22.5	3.4	38	T1-/T2-8MR1

As in the case of Li^+ , empirical interpretation of Na^+ resonances is not possible. Theoretical computations were made by the group of Dr. Štěpán Sklenák. Calculated NMR parameters, i.e. chemical shift and quadrupolar coupling constant, of nine low energy sites of Na^+ compensating negative charge of Al in different T sites are displayed graphically in Figure 6 and compared with experimental values. Three possible low energy Na^+ sites were found for Al in T1 site, two for T2(Al), as same as for T3(Al) and T4(Al). Calculated values of ^{23}Na chemical shift between 0.7 ppm and

-19.9 ppm and quadrupolar coupling constant ranging from 2.6 MHz to 5.7 MHz are in very good agreement with experimental ones ranging from 1.0 ppm to -23.5 ppm and from 0.9 MHz to 5.3 MHz, respectively.

Nevertheless, calculations show, that we are able to distinguish Na in different rings or sites, but not specific Al T site, e.g. that sodium accommodated in one of 8-mr has the same NMR parameters despite Al is in T1 or T3 site. As a consequence, Na^+ cannot be used as a probe of Al siting in the case of ferrierite.

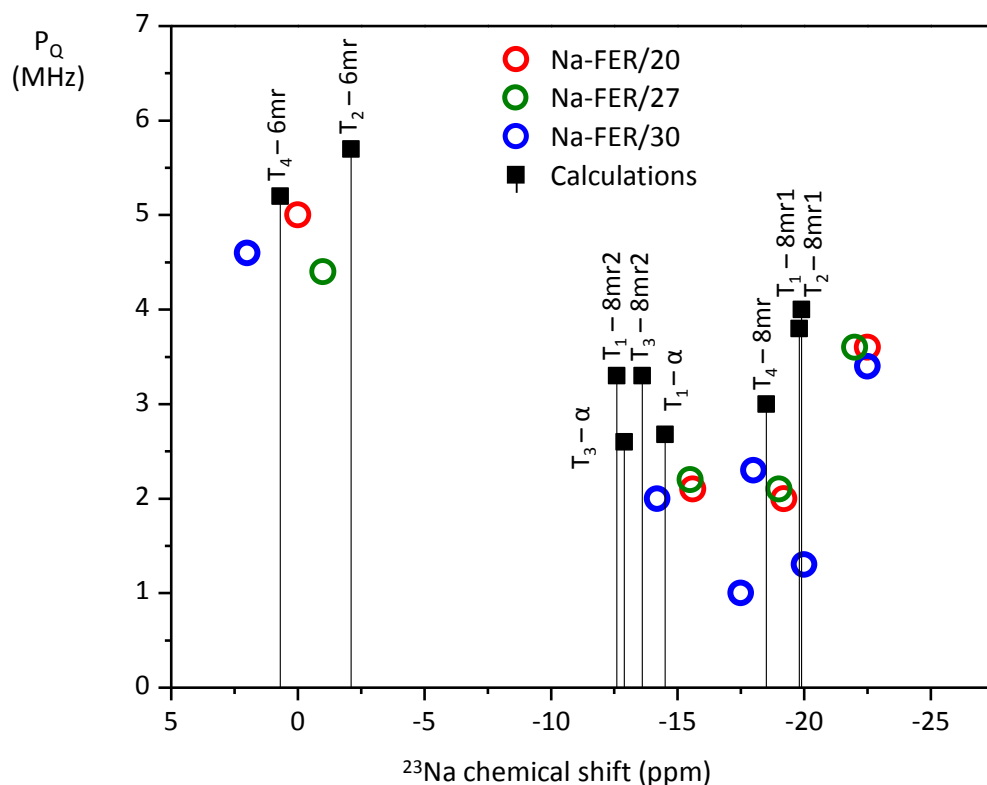


Figure 6 - ^{23}Na chemical shift and quadrupolar product of individual resonances of Na-FER samples compared with calculated values of low-energy Na^+ sites

5.3 Structure of cationic sites in dehydrated CHA as seen by ^{27}Al ssNMR

The single pulse ^{27}Al MAS NMR spectra of the dehydrated as well as hydrated M-CHA (M = Li, Na, and K) samples are compared in Figure 7. The dehydration of the samples is connected with a marked broadening of the ^{27}Al NMR signal. Moreover, this broadening depends on the cation balancing the framework negative charge. Two-dimensional ^{27}Al MQMAS NMR spectra of the dehydrated M-CHA(deh) samples were collected to investigate the mechanism of line broadening in dehydrated zeolites. Note that the collection of the MQ MAS NMR spectrum of an enormously broad signal requires the acquisition time of several days.

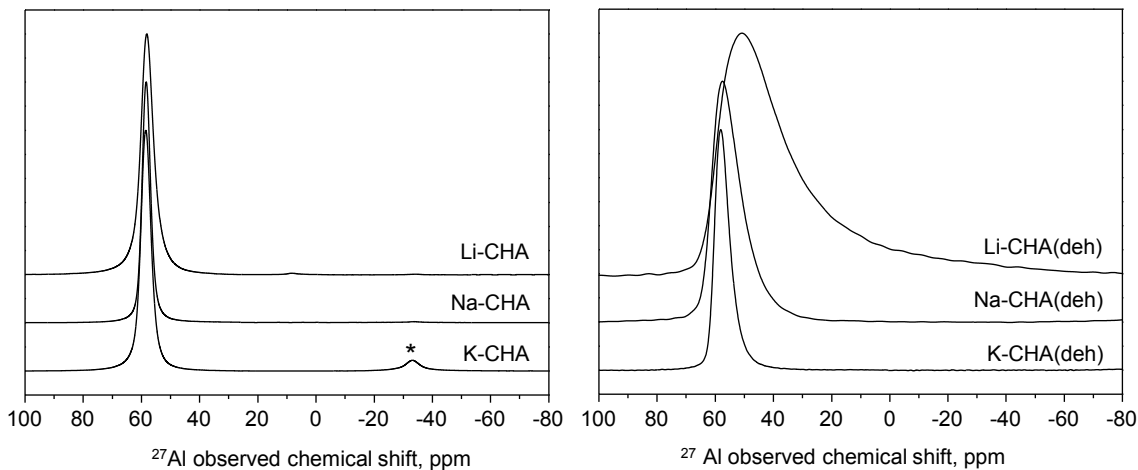


Figure 7 - ^{27}Al MAS NMR spectra of hydrated (left) and dehydrated (right) Li-, Na- and K-CHA

Both the single pulse ^{27}Al MAS and isotropically sheared ^{27}Al 3Q MAS spectra of all the dehydrated samples were simultaneously fitted in the dmfit software using "Czjzek simple" model to obtain the ^{27}Al NMR parameters. ^{27}Al MAS and MQMAS NMR spectra of dehydrated Li-chabazite together with simulations are shown in Figure 8.

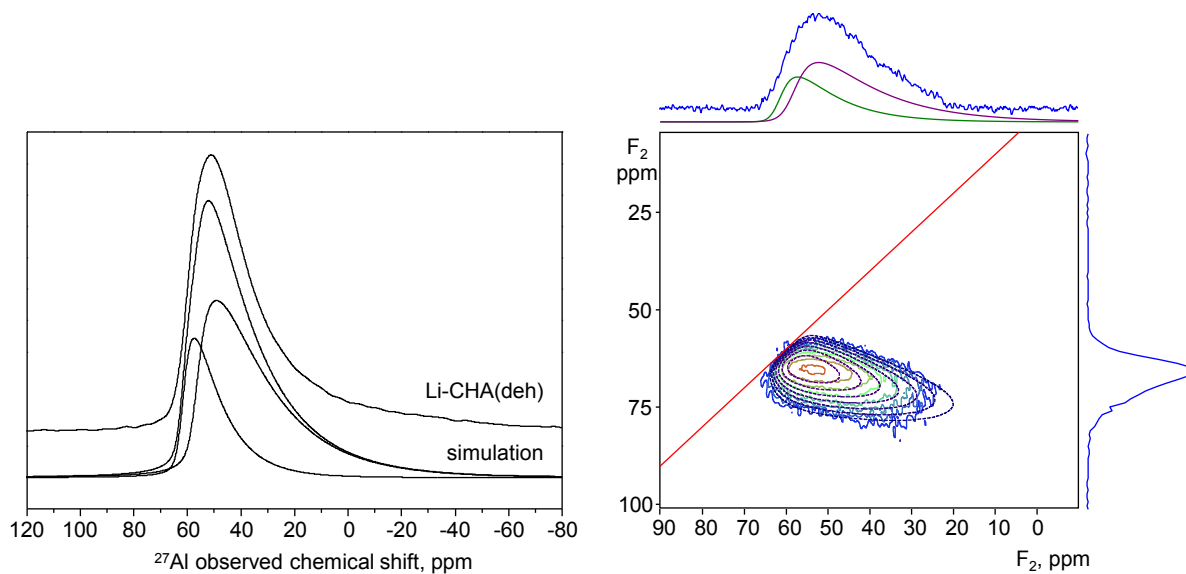


Figure 8 - ^{27}Al MAS (left) and MQMAS (right) NMR spectra of dehydrated Li-, Na- and K-CHA together with simulations

The spectra of the dehydrated Na-CHA and K-CHA samples were simulated using one resonance while two resonances are required for the dehydrated Li-CHA sample. The values of the ^{27}Al isotropic chemical shift and the nuclear quadrupolar coupling parameter P_Q from spectra simulation are shown in Table 4.

Table 4 - ^{27}Al chemical shift (δ), quadrupolar coupling product (P_Q) and relative intensity (I) of individual aluminium resonances of CHA samples

sample	resonance	δ/ppm	P_Q/MHz	$I/\%$
Li-CHA(deh)	I	62.0	5.3	30
	II	57.0	7.3	60
Na-CHA(deh)	I	61.3	4.2	100
K-CHA(deh)	I	60.1	2.9	100
Li-CHA	I	60.0	2.4	100
Na-CHA	I	59.5	1.8	100
K-CHA	I	59.5	1.8	100
K-CHA(190K)	I	59.7	2.1	100

Figure 7 shows well known enormous broadening of the ^{27}Al NMR resonances for the dehydrated samples. The ^{27}Al MAS NMR spectra of the dehydrated M-CHA (M = Li, Na, and K) zeolites significantly differ in their width depending on the cation balancing the negative charge of the AlO_4^- tetrahedra although there is only one crystallographically distinguishable framework T site which could be occupied by Al atoms. The largest broadening (i.e., the largest P_Q values of 5.3 and 7.3 MHz) is observed for the smallest cation Li^+ while the smallest broadening (i.e., the smallest P_Q value of 2.9 MHz) for the largest cation K^+ . The broadening for the Na-CHA sample (i.e., the P_Q value of 4.2 MHz) is in between those for the Li-CHA and K-CHA materials. These results indicate a significant role of the cation interaction with the zeolite framework in the broadening of the ^{27}Al MAS NMR signal upon dehydration of the M-CHA samples.

To elucidate effect of extra-framework cation on ^{27}Al NMR spectrum calculations of the six models of the cationic sites yielded the optimized structures and the corresponding relative energies of the two cationic sites (M^+ accommodated in six-membered and eight-membered rings) were made by Dr. Sklenák's group. The effect of the binding of M^+ to the zeolite framework upon dehydration on the ^{27}Al NMR parameters is composed of two contributions: (i) the change of the local structure of AlO_4^- (i.e., deformation) caused by the binding of M^+ to the zeolite framework without including the effect of the M^+ cation; (ii) the effect of the M^+ cation with the exclusion of the influence of the change of the local structure of AlO_4^- due to the coordination of M^+ to the zeolite framework. The latter could be further investigated employing the background (point) + charge instead of the M^+ cation. These calculations permit the evaluation of the effect of the + charge of the M^+ cation without including the other effects of the M^+ cation.

Comparison of experimental values of quadrupolar product with theoretical calculations (see Figure 9) show that the broadening of the ^{27}Al NMR signals is caused mostly by deformation of AlO_4^- due to the coordination of M^+ to the zeolite framework.

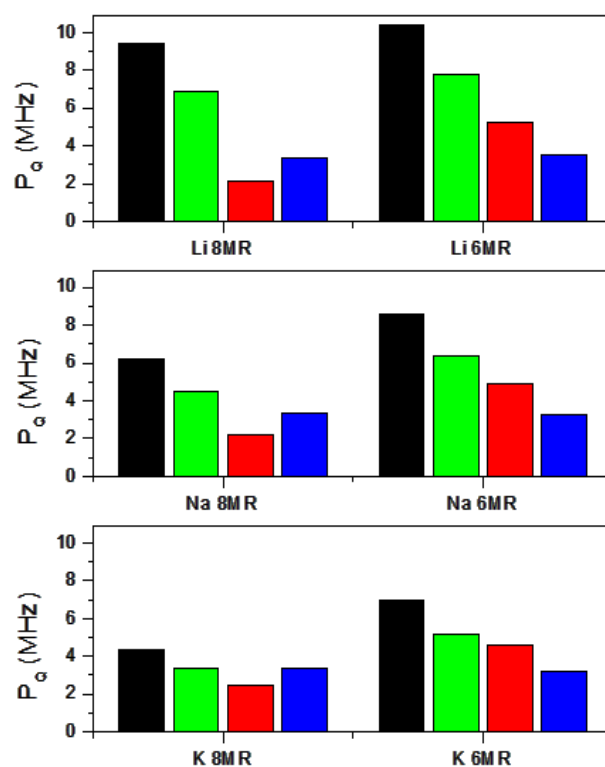


Figure 9 - The calculated P_Q values for (i) the Li^+ -8-ring, Li^+ -6-ring, Na^+ -8-ring, Na^+ -6-ring, K^+ -8-ring, and K^+ -6-ring models (black bars), (ii) the six models with the removed M^+ (green bars), (iii) the bare framework model with the added M^+ cations (red bars), and (iv) the bare framework model with the added + background charges (blue bars)

Conclusions

Presented work demonstrates application of solid-state NMR spectroscopy supported by quantum chemical calculations for analysis of extra-framework sites in zeolites. Quantitative distribution of lithium and sodium cations in crystallographically non-equivalent sites in dehydrated Na- and Li-FER zeolites was determined by combination of advanced techniques of ssNMR. To distinguish crystallographically non-equivalent lithium sites in a narrow range of chemical shifts, a two-dimensional ^7Li - ^7Li correlation EXSY NMR experiment was successfully implemented. Quantitative distribution was subsequently determined by deconvolution of one-dimensional ^7Li MAS NMR spectra. Periodic DFT calculations allowed interpretation of most of the individual lithium resonances. It was found that Li^+ balancing Al in one T site can occupy two different crystallographic positions. On the other hand, assignment of close resonances has to be performed very carefully but still resonances T3 and T4 cannot be distinguished. Sound agreement between results of Li^+ and Al siting opens possibility to use Li^+ as an additional probe of Al siting.

To obtain NMR parameters of broad and overlapping sodium signals in dehydrated Na-FER samples, simultaneous analytical simulation of the ^{23}Na MAS and ^{23}Na MQMAS NMR spectra measured on two different magnetic fields (high and ultra-high) had to be performed. Theoretical calculations revealed that NMR parameters of sodium cations balancing Al in different T sites while located in the same ring are similar. Thus, Na^+ is not a suitable probe of Al siting in the case of ferrierite, yet ^{23}Na ssNMR can provide information about location of sodium in different rings.

It was shown, that both lithium and sodium ssNMR provide useful information about distribution of extra-framework cations. On the other hand, various cationic sites in silicon-rich zeolites have the same chemical environment, so the difference between NMR interaction tensors is only due to the subtle changes of bond lengths and angles. Therefore, some positions would not have been distinguished without analysis of Al siting in the framework. It demonstrates importance of multinuclear approach and thorough analysis of both Al and cation siting for characterization of zeolite catalyst.

Reliability of quantum chemical calculations in predicting structure of extra-framework sites in zeolites has been verified. Calculated NMR parameters are in good agreement with experimental values and allow interpretation of NMR spectra. We suppose that theoretical calculation can be utilized for predicting of cations NMR inactive or difficult to measure (e.g. Cu^+).

To test possibility of indirect characterization of siting of monovalent cations, ^{27}Al MAS and MQMAS NMR spectra of hydrated and dehydrated Li-, Na- and K-CHA samples were recorded. Upon dehydration of the samples, marked broadening of ^{27}Al MAS NMR spectra was observed. Broadening caused by quadrupolar interaction increased with decreasing ionic radius. Sound agreement between experiment and calculations revealed that observed quadrupolar broadening is rather due to the deformation of AlO_4^- tetrahedron by coordination of cation, than due to the effect of positive charge of the cation. Moreover, NMR invisible potassium cation can be identified in ^{27}Al MAS NMR spectrum of dehydrated CHA by Al resonance with magnitude of quadrupolar interaction of about 3 MHz.

List of References

1. Baerlocher, C.; McCusker, L. B., Database of Zeolite Structures.
2. Davis, S.; Inoguchi, Y., *Chemical Economics Handbook, Report, Zeolites*. SRI Consulting: Colorado, 2009.
3. Corma, A.; García, H., Lewis Acids: From Conventional Homogeneous to Green Homogeneous and Heterogeneous Catalysis. *Chemical Reviews* **2003**, *103* (11), 4307-4366.
4. Vermeiren, W.; Gilson, J. P., Impact of Zeolites on the Petroleum and Petrochemical Industry. *Topics in Catalysis* **2009**, *52* (9), 1131-1161.
5. Dědeček, J.; Sobalík, Z.; Wichterlová, B., Siting and Distribution of Framework Aluminium Atoms in Silicon-Rich Zeolites and Impact on Catalysis. *Catalysis Reviews* **2012**, *54* (2), 135-223.
6. Vogt, E. T. C.; Weckhuysen, B. M., Fluid catalytic cracking: recent developments on the grand old lady of zeolite catalysis. *Chemical Society Reviews* **2015**, *44* (20), 7342-7370.

7. Olsbye, U.; Svelle, S.; Lillerud, K. P.; Wei, Z. H.; Chen, Y. Y.; Li, J. F.; Wang, J. G.; Fan, W. B., The formation and degradation of active species during methanol conversion over protonated zeotype catalysts. *Chemical Society Reviews* **2015**, *44* (20), 7155-7176.
8. Primo, A.; Garcia, H., Zeolites as catalysts in oil refining. *Chemical Society Reviews* **2014**, *43* (22), 7548-7561.
9. Olsbye, U.; Svelle, S.; Bjørgen, M.; Beato, P.; Janssens, T. V. W.; Joensen, F.; Bordiga, S.; Lillerud, K. P., Conversion of Methanol to Hydrocarbons: How Zeolite Cavity and Pore Size Controls Product Selectivity. **2012**, *51* (24), 5810-5831.
10. Skalska, K.; Miller, J. S.; Ledakowicz, S., Trends in NO_x abatement: A review. *Science of The Total Environment* **408** (19), 3976-3989.
11. Pérez-Ramírez, J.; Kapteijn, F.; Schöffel, K.; Moulijn, J. A., Formation and control of N₂O in nitric acid production: Where do we stand today? *Applied Catalysis B: Environmental* **2003**, *44* (2), 117-151.
12. Beale, A. M.; Gao, F.; Lezcano-Gonzalez, I.; Peden, C. H. F.; Szanyi, J., Recent advances in automotive catalysis for NO_x emission control by small-pore microporous materials. *Chemical Society Reviews* **2015**, *44* (20), 7371-7405.
13. Espeel, In *Catalysis and zeolites*, Weitkamp; Puppe, Eds. Springer: Berlin, 1999.
14. Ennaert, T.; Van Aelst, J.; Dijkmans, J.; De Clercq, R.; Schutyser, W.; Dusselier, M.; Verboekend, D.; Sels, B. F., Potential and challenges of zeolite chemistry in the catalytic conversion of biomass. *Chemical Society Reviews* **2016**, *45* (3), 584-611.
15. Tang, P.; Zhu, Q.; Wu, Z.; Ma, D., Methane activation: the past and future. *Energy & Environmental Science* **2014**, *7* (8), 2580-2591.
16. Sakakura, T.; Choi, J.-C.; Yasuda, H., Transformation of Carbon Dioxide. *Chemical Reviews* **2007**, *107* (6), 2365-2387.
17. Perego, C.; Carati, A.; Ingallina, P.; Mantegazza, M. A.; Bellussi, G., Production of titanium containing molecular sieves and their application in catalysis. *Applied Catalysis A: General* **2001**, *221*, 63-72.
18. Pirutko, L. V.; Chernyavsky, V. S.; Uriarte, A. K.; Panov, G. I., Oxidation of benzene to phenol by nitrous oxide: Activity of iron in zeolite matrices of various composition. *Applied Catalysis A: General* **2002**, *227* (1), 143-157.
19. Panov, G. I.; Kharitonov, A. S.; Sobolev, V. I., Oxidative hydroxylation using dinitrogen monoxide: a possible route for organic synthesis over zeolites. *Applied Catalysis A: General* **1993**, *98* (1), 1-20.
20. Lim, K. H.; Grey, C. P., Characterization of Extra-Framework Cation Positions in Zeolites NaX and NaY with Very Fast ²³Na MAS and Multiple Quantum MAS NMR Spectroscopy. *Journal of the American Chemical Society* **2000**, *122* (40), 9768-9780.
21. Mortier, W. J., *Compilation of Extra-framework Sites in Zeolites*. Butterworths: Guildford, 1982.
22. Olson, D. H.; Khosrovani, N.; Peters, A. W.; Toby, B. H., Crystal Structure of Dehydrated CsZSM-5 (5.8Al): Evidence for Nonrandom Aluminum Distribution. *The Journal of Physical Chemistry B* **2000**, *104* (20), 4844-4848.

23. Mentzen, B. F., Crystallographic Determination of the Positions of the Monovalent H, Li, Na, K, Rb, and Tl Cations in Fully Dehydrated MFI Type Zeolites. *The Journal of Physical Chemistry C* **2007**, *111* (51), 18932-18941.
24. Dalconi, M. C.; Alberti, A.; Cruciani, G.; Ciambelli, P.; Fonda, E., Siting and coordination of cobalt in ferrierite: XRD and EXAFS studies at different Co loadings. *Microporous and Mesoporous Materials* **2003**, *62* (3), 191-200.
25. Dalconi, M. C.; Cruciani, G.; Alberti, A.; Ciambelli, P.; Rapacciuolo, M. T., Ni²⁺ ion sites in hydrated and dehydrated forms of Ni-exchanged zeolite ferrierite. *Microporous and Mesoporous Materials* **2000**, *39* (3), 423-430.
26. Kim, C. W.; Heo, N. H.; Seff, K., Framework Sites Preferred by Aluminum in Zeolite ZSM-5. Structure of a Fully Dehydrated, Fully Cs⁺-Exchanged ZSM-5 Crystal (MFI, Si/Al = 24). *The Journal of Physical Chemistry C* **2011**, *115* (50), 24823-24838.
27. Dědeček, J.; Kaucký, D.; Wichterlová, B., Co²⁺ ion siting in pentasil-containing zeolites, part 3.: Co²⁺ ion sites and their occupation in ZSM-5: a VIS diffuse reflectance spectroscopy study. *Microporous and Mesoporous Materials* **2000**, *35 - 36*, 483-494.
28. Kaucký, D.; Dědeček, J.; Wichterlová, B., Co²⁺ ion siting in pentasil-containing zeolites: II. Co²⁺ ion sites and their occupation in ferrierite. A VIS diffuse reflectance spectroscopy study. *Microporous and Mesoporous Materials* **1999**, *31*, 75-87.
29. Nachtigall, P.; Delgado, M. R.; Nachtigalova, D.; Arean, C. O., The nature of cationic adsorption sites in alkaline zeolites—single, dual and multiple cation sites. *Physical Chemistry Chemical Physics* **2012**, *14* (5), 1552-1569.
30. Hunger, M., Solid-State NMR Spectroscopy. In *Zeolite Characterization and Catalysis: A Tutorial*, Chester, A. W.; Derouane, E. G., Eds. Springer Netherlands: Dordrecht, 2009; pp 65-105.
31. Pyykko, P., Spectroscopic nuclear quadrupole moments. *Molecular Physics* **2001**, *99* (19), 1617-1629.
32. Hunger, M.; Engelhardt, G.; Koller, H.; Weitkamp, J., CHARACTERIZATION OF SODIUM-CATIONS IN DEHYDRATED FAUJASITES AND ZEOLITE EMT BY NA-23 DOR, 2D-NUTATION, AND MAS NMR. *Solid State Nuclear Magnetic Resonance* **1993**, *2* (3), 111-120.
33. Feuerstein, M.; Hunger, M.; Engelhardt, G.; Amoureux, J. P., Characterisation of sodium cations in dehydrated zeolite NaX by Na-23 NMR spectroscopy. *Solid State Nuclear Magnetic Resonance* **1996**, *7* (2), 95-103.
34. Ganapathy, S.; Das, T. K.; Vetrivel, R.; Ray, S. S.; Sen, T.; Sivasanker, S.; Delevoye, L.; Fernandez, C.; Amoureux, J. P., Anisotropic Chemical Shielding, M-Site Ordering, and Characterization of Extraframework Cations in ETS-10 Studied through MAS/MQ-MAS NMR and Molecular Modeling Techniques. *Journal of the American Chemical Society* **1998**, *120* (19), 4752-4762.
35. Hunger, M.; Sarv, P.; Samoson, A., Two-dimensional triple-quantum Na-23 MAS NMR spectroscopy of sodium cations in dehydrated zeolites. *Solid State Nuclear Magnetic Resonance* **1997**, *9* (2-4), 115-120.
36. Caldarelli, S.; Buchholz, A.; Hunger, M., Investigation of Sodium Cations in Dehydrated Zeolites LSX, X, and Y by ²³Na Off-Resonance RIACT Triple-

- Quantum and High-Speed MAS NMR Spectroscopy. *Journal of the American Chemical Society* **2001**, *123* (29), 7118-7123.
37. Dedecek, J.; Lucero, M. J.; Li, C.; Gao, F.; Klein, P.; Urbanova, M.; Tvaruzkova, Z.; Sazama, P.; Sklenak, S., Complex Analysis of the Aluminum Siting in the Framework of Silicon-Rich Zeolites. A Case Study on Ferrierites. *Journal of Physical Chemistry C* **2011**, *115* (22), 11056-11064.
 38. Ernst, H.; Freude, D.; Wolf, I., MULTINUCLEAR SOLID-STATE NMR-STUDIES OF BRONSTED SITES IN ZEOLITES. *Chemical Physics Letters* **1993**, *212* (6), 588-596.
 39. Freude, D.; Ernst, H.; Wolf, I., SOLID-STATE NUCLEAR-MAGNETIC-RESONANCE STUDIES OF ACID SITES IN ZEOLITES. *Solid State Nuclear Magnetic Resonance* **1994**, *3* (5), 271-286.
 40. Jiao, J.; Altwasser, S.; Wang, W.; Weitkamp, J.; Hunger, M., State of aluminum in dealuminated, nonhydrated zeolites Y investigated by multinuclear solid-state NMR spectroscopy. *Journal of Physical Chemistry B* **2004**, *108* (38), 14305-14310.
 41. Jiao, J.; Kanellopoulos, J.; Wang, W.; Ray, S. S.; Foerster, H.; Freude, D.; Hunger, M., Characterization of framework and extra-framework aluminum species in non-hydrated zeolites Y by Al-27 spin-echo, high-speed MAS, and MQMAS NMR spectroscopy at B₀=9.4 to 17.6 T. *Physical Chemistry Chemical Physics* **2005**, *7* (17), 3221-3226.
 42. Clark Stewart, J.; Segall Matthew, D.; Pickard Chris, J.; Hasnip Phil, J.; Probert Matt, I. J.; Refson, K.; Payne Mike, C., First principles methods using CASTEP. In *Zeitschrift für Kristallographie - Crystalline Materials*, 2005; Vol. 220, p 567.
 43. Bonhomme, C.; Gervais, C.; Babonneau, F.; Coelho, C.; Pourpoint, F.; Azaïs, T.; Ashbrook, S. E.; Griffin, J. M.; Yates, J. R.; Mauri, F.; Pickard, C. J., First-Principles Calculation of NMR Parameters Using the Gauge Including Projector Augmented Wave Method: A Chemist's Point of View. *Chemical Reviews* **2012**, *112* (11), 5733-5779.
 44. Dedecek, J.; Wichterlova, B.; Kubat, P., Siting of the Cu⁺ ions in dehydrated ion exchanged synthetic and natural chabasites: a Cu⁺ photoluminescence study. *Microporous and Mesoporous Materials* **1999**, *32* (1-2), 63-74.
 45. Massiot, D.; Fayon, F.; Capron, M.; King, I.; Le Calvé, S.; Alonso, B.; Durand, J.-O.; Bujoli, B.; Gan, Z.; Hoatson, G., Modelling one- and two-dimensional solid-state NMR spectra. **2002**, *40* (1), 70-76.
 46. Klein, P.; Dedecek, J.; Thomas, H. M.; Whittleton, S. R.; Pashkova, V.; Brus, J.; Kobera, L.; Sklenak, S., NMR crystallography of monovalent cations in inorganic matrixes: Li⁺ siting and the local structure of Li⁺ sites in ferrierites. *Chemical Communications* **2015**, *51* (43), 8962-8965.

List of Students' Published Works

Publications related to the subject of dissertation:

Dedecek, J., Lucero, M. J., Li, C., Gao, F., Klein, P., Urbanova, M., Tvaruzkova, Z., Sazama, P., Sklenak, S. Complex Analysis of the Aluminum Siting in the Framework of Silicon-Rich Zeolites. A Case Study on Ferrierites. *Journal of Physical Chemistry C*, 2011, 115, 22, 11056-11064.

Klein P., Dedecek J., Thomas H.M., Whittleton S.R., Pashkova V., Brus J., Kobera L., Sklenak S., NMR crystallography of monovalent cations in inorganic matrixes: Li⁺ siting and the local structure of Li⁺ sites in ferrierites, *Chemical Communications*, 51 (43), 8962-8965, 2015

Klein P., Pashkova V., Thomas H.M., Whittleton S.R., Brus J., Kobera L., Dedecek J., Sklenak S., Local Structure of Cationic Sites in Dehydrated Zeolites Inferred from ²⁷Al Magic-Angle Spinning NMR and Density Functional Theory Calculations. A Study on Li-, Na-, and K-Chabazite, *Journal of Physical Chemistry C*, 120, 26, 14216–14225, 2016

Further publications:

Synthesis of ZSM-5 Zeolites with Defined Distribution of Al Atoms in the Framework and Multinuclear MAS NMR Analysis of the Control of Al Distribution, Jiri Dedecek, Vendula Balgová, Veronika Pashkova, Petr Klein, Blanka Wichterlová, *Chemistry of Materials* 24 (16), 3231-3239, 2012

Alkali-bonded ceramics with hierarchical tailored porosity, E. Landi, V. Medri, E. Papa, J. Dedecek, P. Klein, P. Benito, A. Vaccari, *Applied Clay Science* 73, 56-64, 2013

Acid and redox activity of template-free Al-rich H-BEA* and Fe-BEA* zeolites, Petr Sazama, Blanka Wichterlová, Štěpán Sklenák, Vasile I. Parvulescu, Natalia Candu, Galina Sádovská, Jiří Dědeček, Petr Klein, Veronika Pashkova, Petr Šťastný, *Journal of Catalysis*, 318, 22-33, 2014

Biaxial Q-shearing of ²⁷Al 3QMAS NMR spectra: Insight into the structural disorder of framework aluminosilicates, L. Kobera, J. Brus, P. Klein, J. Dedecek, M. Urbanova, *Solid state nuclear magnetic resonance* 57, 29-38, 2014

Tailoring of the structure of Fe-cationic species in Fe-ZSM-5 by distribution of Al atoms in the framework for N₂O decomposition and NH₃-SCR-NO_x, Petr Sazama, Blanka Wichterlová, Edyta Tábor, Petr Šťastný, Naveen K Sathu, Zdeněk Sobalík, Jiří Dědeček, Štěpán Sklenák, Petr Klein, Alena Vondrová, *Journal of Catalysis* 312, 123-138, 2014

Incorporation of Al at ZSM-5 in hydrothermal synthesis. Tuning of Al pairs in the framework, V. Pashkova, P. Klein, J. Dedecek, V. Tokarová, B. Wichterlová, *Microporous and Mesoporous Materials*, 202, 138-146, 2015

Structure of Framework Aluminum Lewis Sites and Perturbed Aluminum Atoms in Zeolites as Determined by ^{27}Al 1H REDOR (3Q) MAS NMR Spectroscopy and DFT/Molecular Mechanics, Jiří Brus, Libor Kobera, Wolfgang Schoefberger, Martina Urbanová, Petr Klein, Petr Sazama, Edyta Tabor, Stepan Sklenak, Anna V Fishchuk, Jiří Dědeček, *Angewandte Chemie International Edition*, 54 (2), 541-545, 2015

Al-rich beta zeolites. Distribution of Al atoms in the framework and related protonic and metal-ion species, P Sazama, E Tabor, P Klein, B Wichterlova, S Sklenak, L Mokrzycki, V Pashkova, M Ogura, J Dedecek
Journal of Catalysis 333, 102-114

Location of Framework Al Atoms in the Channels of ZSM-5: Effect of the (Hydrothermal) Synthesis
V Pashkova, S Sklenak, P Klein, M Urbanova, J Dědeček
Chemistry—A European Journal 22 (12), 3937-3941

Remarkably enhanced density and specific activity of active sites in Al-rich Cu-, Fe- and Co-beta zeolites for selective catalytic reduction of NO_x
P Sazama, R Pilar, L Mokrzycki, A Vondrova, D Kaucky, J Plsek, Stepan Sklenak, Petr Stastny, Petr Klein
Applied Catalysis B: Environmental 189, 65-74

Superior activity of non-interacting close acidic protons in Al-rich Pt/H-^{*} BEA zeolite in isomerization of *n*-hexane
P Sazama, D Kaucky, J Moravkova, R Pilar, P Klein, J Pastvova, E Tabor, S Sklenak, I Jakubec, L Mokrzycki
Applied Catalysis A: General 533, 28-37

TNU-9 Zeolite: Aluminum Distribution and Extra-Framework Sites of Divalent Cations, R Karcz, J Dedecek, B Supronowicz, HM Thomas, P Klein, E Tabor, P Sazama, V Pashkova, S Sklenak
Chemistry—A European Journal 23 (37), 8857-8870

Effect of Enhanced Accessibility of Acid Sites in Micromesoporous Mordenite Zeolites on Hydroisomerization of *n*-Hexane
J Pastvova, D Kaucky, J Moravkova, J Rathousky, S Sklenak, M Vorokhta, L Brabec, R Pilar, I Jakubec, E Tabor, P Klein, P Sazama
ACS Catalysis 7 (9), 5781-5795

Catalytic Properties of 3D Graphene-Like Microporous Carbons Synthesized in a Zeolite Template, P Sazama, J Pastvova, C Rizescu, A Tirsoaga, VI Parvulescu, H Garcia, L Kobera, J Seidel, J Rathousky, P Klein, I Jirka, J Moravkova, V Blechta
ACS Catalysis 8 (3), 1779-1789